ISBN: 978-3-95450-261-5 ISSN: 2673-7000 doi: 10.18429/JACoW-NAPAC2025-THYD01

COLLECTIVE EFFECTS: CHALLENGES AND SOLUTIONS FOR THE EIC PROJECT*

A. Blednykh†
Brookhaven National Laboratory, Upton, NY, USA

Abstract

The Electron-Ion Collider (EIC) project at Brookhaven National Laboratory aims to deliver groundbreaking insights into the fundamental structure of matter through high-energy collisions involving electrons, ions, protons, or helium-3 nuclei. Achieving the desired luminosity and maintaining stability in this complex accelerator environment pose significant challenges, particularly concerning impedance and collective effects. One such challenge is ensuring beam stability during electron cooling at the injection energy in the Hadron Storage Ring (HSR) to effectively mitigate proton emittance growth. Potential solutions include advanced simulation techniques using the ELEGANT code and applying the Haissinski solution for the proton beam to determine single-bunch instability thresholds, both with and without a second harmonic cavity.

INTRODUCTION

The Electron-Ion Collider (EIC) is a next-generation accelerator facility under construction at Brookhaven National Laboratory, designed to collide polarized electrons with polarized protons and heavy ions at high luminosity and variable center-of-mass energies [1]. The EIC complex comprises multiple accelerator stages (Fig. 1), including a DC photoelectron gun, a 750 MeV S-band LINAC, the Beam Accumulator Ring (BAR, 750 MeV) – with design led by the NSLS-II team - the Rapid Cycling Synchrotron (RCS, 0.750→18 GeV), and two high-energy storage rings: the Electron Storage Ring (ESR) and the Hadron Storage Ring (HSR). Electrons are accelerated in the RCS from 0.750 GeV to 5, 10, or 18 GeV and subsequently injected into the ESR at the corresponding energy. Hadrons are injected into the HSR at 23.8 GeV and ramped to their final energies - ranging from 41 to 275 GeV - depending on the species, including protons (p), ions, or He^3.

The goal of the EIC is to deliver a design luminosity of up to 10^{33}-10^{34} $cm^{-2}s^{-1}$, enabled by advanced features such as beam cooling systems, a 25 mrad crab crossing angle, high beam currents - up to I_{av}=2.5 A with M=1160 bunches of σ_s~7 mm length in the ESR, and up to 0.7 A / 1 A with M=290 and M=1160 bunches of σ_s~60 mm in the HSR during storage. At injection energy, the bunch length in the HSR is expected to be significantly longer, around σ_s~1.5 m. Since the collective effects topic in the EIC project covers multiple ring accelerators, this paper focuses on single-bunch stability at injection energy and the associated contributions from coupling impedance and space charge impedance in the HSR.

* Work supported by Brookhaven Science Associates, LLC under Contract No. DE-SC0012704 and DE-AC02-06CH11357 with the U.S. Department of Energy.
† blednykh@bnl.gov

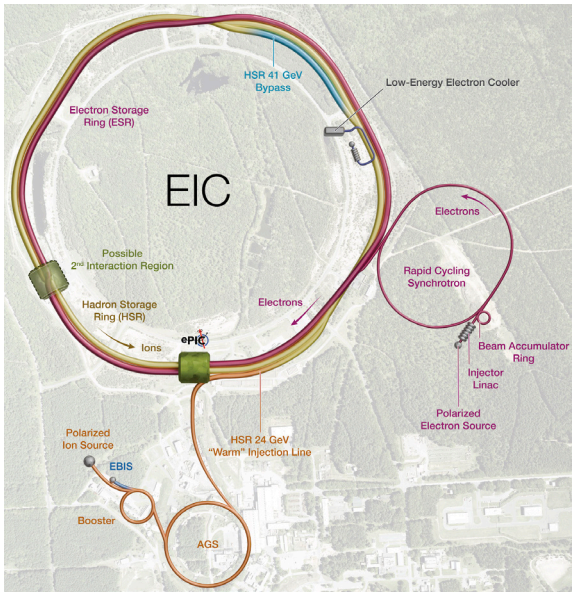

Figure 1: Top view schematic of the Electron-Ion Collider (EIC) accelerator complex, including the electron and hadron injector chains, the Beam Accumulator Ring (BAR), the Rapid Cycling Synchrotron (RCS), and the Electron and Hadron Storage Rings (ESR and HSR).

HSR

Table 1 presents the HSR beam intensity parameters at different energies, based on species acceleration. In this paper, single-bunch (SB) stability in the HSR is studied at the injection energy of 23.8 GeV, where the combination of long bunches ($\sigma_\tau \approx 5\,ns$), achieved using second harmonic RF cavity (49.2 MHz), and high peak current (~3.5 A), presents significant collective effects challenges for maintaining low horizontal and vertical emittances achieved by electron cooling [2]. The HSR beam screen, shown in Fig. 2, consists of an amorphous carbon–coated, copper-clad stainless-steel pipe inserted into the existing RHIC stainless steel vacuum chambers, primarily within the arc sections. The beam screen is actively cooled and is expected to operate at cryogenic temperatures, ~4 K.

The profile of the HSR vacuum chamber varies along straight sections depending on the requirements of the associated subsystems. In IR2, the vacuum chamber is designed to accommodate the low-energy electron cooler [2]. In IR4, the normal-conducting RF cavities and injection stripline kickers are installed. IR6 houses the ePIC detector chamber, where the hadron and electron beam pipes merge into a common section. This region requires careful

ISBN: 978-3-95450-261-5 ISSN: 2673-7000 doi: 10.18429/JACoW-NAPAC2025-THYD01

Table 1: HSR Beam Intensity Parameters

Energy, E (GeV)	**23.8**	**41**	**100/110**	**275**
Bunch length, σ_τ (ps)	4975*	250	234	200
Average current, I_{av} (A)	1	0.38	0.69/1	0.69/1
Number of bunches, M	290	1160	1160	290/1160
Number of hadrons per bunch, N	$2.8\text{x}10^{11}$	$2.6\text{x}10^{10}$	$4.8\text{x}10^{10}/6.9\text{x}10^{10}$	$19\text{x}10^{10}/6.9\text{x}10^{10}$
Bunch charge, Nh (nC)	44.8	4.2	7.6/11	30.4/11
Single bunch current, $I_0 = \frac{Nh}{T_0}$ (mA)	3.5	0.3	0.6/0.9	2.4/0.9
Peack bunch current, $I_p = \frac{Nh}{\sqrt{2\pi}\sigma_\tau}$ (A)	3.5	7	13/19	61/22

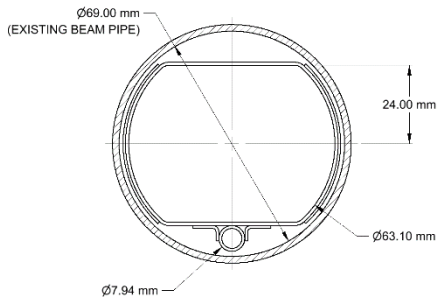

Figure 2: HSR beam screen vacuum chamber profile in the arcs, with a vertical half-aperture of 24 mm and a horizontal half-aperture of ~32 mm.

mechanical and electromagnetic design to minimize impedances. IR10 contains the superconducting RF (SRF) system, requiring a vacuum chamber designed to interface with cryomodules and accommodate higher-order mode (HOM) absorbers. Lastly, IR12 is reserved for the stochastic cooling system.

Table 2 shows the beam parameters at the injection energy of 23.8 GeV for HSR. Low-energy electron cooling is applied to minimize proton transverse emittances, enabling the high luminosity required for the physics program. Before cooling, the normalized transverse emittances are $\varepsilon_{x,y}\gamma_0 \approx 2.5$ μm. After cooling, the emittances are reduced to $\varepsilon_x\gamma_0 \approx 0.5$ μm and $\varepsilon_y\gamma_0 \approx 0.3$ μm. These reductions in emittance lead to smaller beam sizes, decreasing from $\sigma_{x,y} \approx 1.5\ mm$ before cooling to $\sigma_x \approx 0.66\ mm$ and $\sigma_y \approx 0.52\ mm$ after cooling, based on the average beta functions $< \beta_x >= 22.4\ m$ and $< \beta_y >= 23.3\ m$. Using these post-cooling beam parameters, space charge effects were studied along with geometric and resistive wall wakefields/impedances, simulated separately using the ECHO 2D [3], ECHO 3D [4], and GdfidL [5] codes.

Analytical predictions by A. Burov, based on Refs. [6,7], indicate potential longitudinal single-bunch instabilities driven by both longitudinal space charge and geometric coupling impedance. To investigate this, longitudinal and transverse beam dynamics have been studied using the ELEGANT [8] and TRANFT [9] particle tracking codes. To evaluate vertical beam stability, the nonlinear transverse space charge (TSC) impedance has been implemented into ELEGANT by M. Borland for single-bunch tracking simulations, enabling detailed analysis of tune shifts and emittance growth driven by space charge and wakefield interactions.

Table 2: Beam Parameters at Injection Energy

Energy, E (GeV)	**23.8**	
Circumference, C (m)	3833.93	
Lorentz Factor, γ_0	25.36	
Transition Energy, γ_t	22.7	
Energy Spread, σ_δ	$7.4\text{x}10^{-4}$	
RF System, 24.6 MHz (h=315), V_{RF} (MV)	0.040	
Bunch Length, σ_τ (ns) / σ_s (m)	3.472 / 1.04	
Cooling	Before	After
Vertical beam size, σ_y (mm)	1.5	0.52
Horizontal beam size, σ_x (mm)	1.5	0.66

LONGITUDINAL BEAM STABILITY

To study longitudinal beam dynamics at injection energy, the longitudinal space charge (LSC) impedance and corresponding pseudo-Green function were used as inputs for ELEGANT tracking simulations. The LSC impedance (Eq. 1) and wakefield (Eq. 2) expressions, based on analytical formulations from A. Chao [10] and extended in subsequent work, were evaluated for a Gaussian bunch profile with an RMS length of 4 mm [11]:

$$Z_{||}(\omega) = -i\frac{\omega}{c}\frac{Z_0}{2\pi}\frac{C}{\gamma_0^2}\left(ln\frac{b}{\sigma_\perp}+\frac{1}{2}\right) \quad (1)$$

$$w_c(z) = -\frac{Z_0 c}{2\pi^{3/2}}\frac{C}{\gamma_0^2\sigma_s}\left(ln\frac{b}{\sigma_\perp}+\frac{1}{2}\right)\frac{z}{\sigma_s^2}\exp\left(-z^2/2\sigma_s^2\right), \quad (2)$$

where b is the vacuum chamber radius, $\sigma_\perp$ is the transverse beam size, C is the ring circumference, γ_0 is the Lorentz factor, and Z_0 is the impedance of free space. The imaginary part of the longitudinal space charge (LSC) impedance divided by n, where $n = \omega/\omega_0$, is $(ImZ/n)_0 = 2.6\ \Omega$ calculated for $C = 3833.93\ m$, $\gamma_0 = 25.4$, $b = 32\ mm$, and $\sigma_x = 0.66\ mm$. The imaginary part of the longitudinal

ISBN: 978-3-95450-261-5 ISSN: 2673-7000 doi: 10.18429/JACoW-NAPAC2025-THYD01

space charge (LSC) impedance increases linearly with frequency; therefore, the normalized quantity ImZ/n remains approximately constant over a wide frequency range. In Fig. 3, the LSC wakefield is plotted for a 4 mm bunch length. Its sign convention is opposite to that of the total longitudinal geometric (GM) and resistive wall (RW) wakefields shown in Fig. 4.

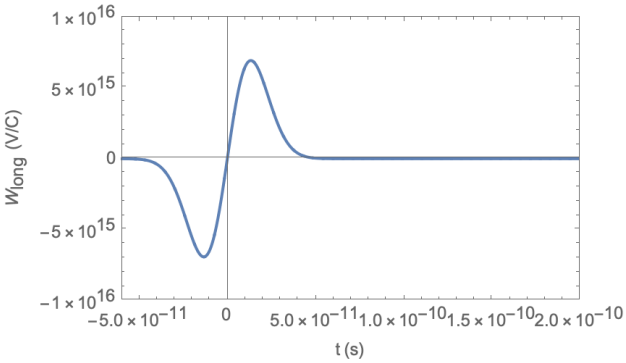

Figure 3: Longitudinal space charge (LSC) wakefield for a 4 mm RMS bunch length.

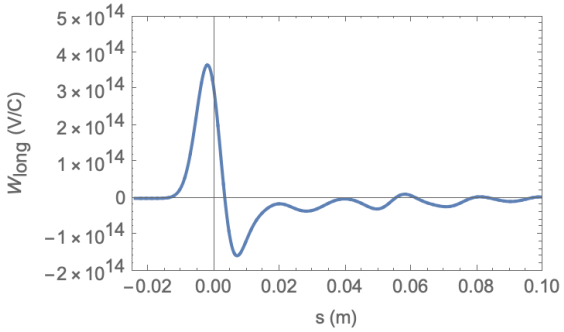

Figure 4: Total longitudinal geometric (GM) and resistive wall (RW) wakefield for a 4 mm RMS bunch length.

The real and imaginary parts of the longitudinal impedance are presented in Fig. 5 for SC and GM+RW. The left plot shows that the real part, $ReZ_{||}(\omega) = 0$, is zero for the space charge impedance (wine line), while the GM+RW impedance (green line) increases with frequency due to resonances from vacuum chamber components and material properties. This real part of the impedance is used to evaluate the beam-induced heating of HSR vacuum components under worst-case conditions: $I_{av} = 0.69\,A$ within $M = 290$ bunches, a bunch length of $\sigma_\tau = 200\,ps$ and a radial orbit shift of 23 mm in the arcs. The imaginary part, $ImZ_{||}(\omega)$ (right plot), shows that the LSC impedance from Eq. 1, with high-frequency filtering applied (super-Gaussian), dominates over the GM+RW contribution. Due to their opposite sign, the LSC impedance causes bunch shortening, whereas the total geometric (GM) and resistive wall (RW) impedances lead to bunch lengthening. To perform longitudinal beam dynamics simulations in ELEGANT, the Haissinski equilibrium distribution [12] was applied at various beam intensities for the proton beam, incorporating both LSC and GM+RW impedances. The Haissinski solver developed by R. Lindberg was used to compute the equilibrium distribution based on the specified impedances and to generate a corresponding particle file for use in ELEGANT.

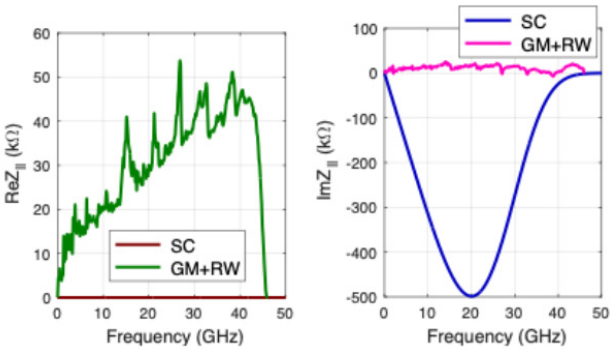

Figure 5: Real and imaginary parts of the LSC and geometric (GM) and resistive wall (RW) impedance.

The Haissinski solution provides a self-consistent description of the longitudinal equilibrium distribution under the influence of collective effects and RF forces. Although originally developed for electron beams, it can also be applied to hadron beams - such as protons - provided that specific considerations are taken into account. For proton beams, synchrotron radiation damping is negligible, and the dominant effects shaping the longitudinal distribution arise from space charge (SC) and geometric plus resistive wall (GM+RW) impedances. In the context of the EIC, where electron cooling is employed, the beam can reach a quasi-equilibrium state, justifying the application of the Haissinski solution. Physically, the Haissinski distribution is meaningful if the energy spread and collective forces are known, the longitudinal distribution becomes a function of the single-particle Hamiltonian H allowing one to compute a more accurate equilibrium solution. These considerations together validate the use of the Haissinski solution for proton beams in the HSR at injection energy.

For the LSC impedance, the Haissinski equation takes the following form [13]:

$$F(q) = \exp\left(-\frac{q^2}{2} + \frac{eI_0Z_0C\,(0.5 + \ln(b/\sigma))}{2\pi E_0\eta_s\sigma_\delta^2\gamma^2\sigma_{z0}}\frac{F(q)}{\int dqF(q)}\right) = \exp\left(-\frac{q^2}{2} + P_{SC}\frac{F(q)}{\int dqF(q)}\right) \quad (3)$$

where $q = z/\sigma_{z0}$ and σ_{z0} is the natural bunch length without wakefields. The analytical form incorporates both the RF potential and the self-induced potential from the LSC impedance. An equilibrium solution exists as $P_{SC} \leq P_{SC,max} \approx 1.55$. This threshold defines the maximum current for which a stable stationary solution can be found. For the HSR proton beam case, the Haissinski equilibrium is valid up to 5 mA with LSC impedance alone (Fig. 6), and extends up to 8 mA when the total impedance (SC+GM+RW) is included (Fig. 7). This range comfortably exceeds the nominal single-bunch current $I_0 = 3.5$ mA at injection.

ISBN: 978-3-95450-261-5 ISSN: 2673-7000 doi: 10.18429/JACoW-NAPAC2025-THYD01

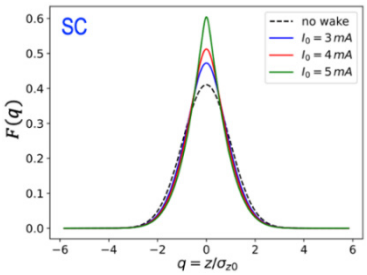

Figure 6: Beam profiles at various single-bunch currents for the LSC. The bunch profile becomes more peaked and compressed at 5 mA.

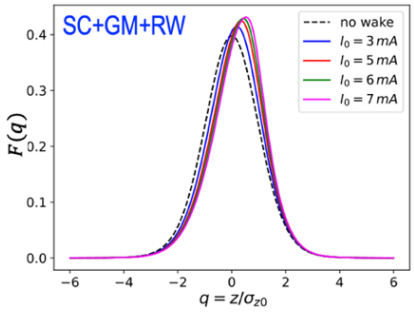

Figure 7: Beam profiles at various single-bunch currents including SC+GM+RW impedances. The stationary Haissinski solution exists up to 8 mA.

The particle tracking simulations using computed beam profiles are shown in Fig. 8 and Fig. 9 presenting the energy spread and bunch length as a function of the number of turns, including SC+GM+RW impedances. For beam currents up to 6 mA, both parameters remain stable, indicating a longitudinal equilibrium state. At a single-bunch current of 8 mA, a rapid increase in energy spread is observed, indicating that the beam becomes unstable. This behavior suggests that the microwave instability (MWI) threshold is ~7 mA for the given wakefields and impedances (SC + GM + RW). By introducing a second harmonic RF cavity operating at 49.2 MHz with $V_{RF} = 20\,kV$, the longitudinal bunch profile is extended, leading to reduced peak charge density. When considering only the LSC impedance, the Haissinski steady-state current limit increases from 5 mA to 10 mA - effectively doubling the accessible current range (Fig. 10). For the total longitudinal impedance (SC+GM+RW), the solution is extended from 8 mA to 12 mA, representing an increase by a factor of ~1.5. The particle tracking simulations are presented in Fig. 11 for the energy spread and in Fig. 12 for the bunch length, using the double-RF system with combined SC + GM + RW impedances. Both the energy spread, and bunch length increase monotonically and reach steady-state values. There is no clear evidence of microwave instability (MWI) within this current range, allowing us to predict that the MWI threshold is greater than the nominal single-bunch current of $I_0 =$ 3.5 mA. At this current, the energy spread is expected to remain close to the design value, consistent with the requirements imposed by the cooling beam parameters.

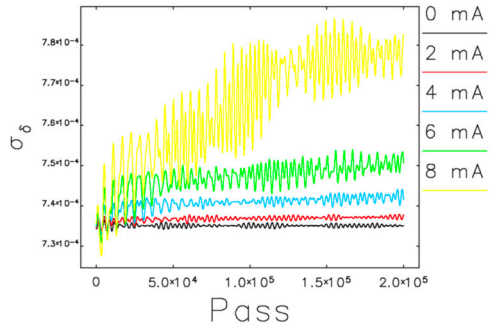

Figure 8: Energy spread vs. number of turns for different single-bunch currents with SC+GM+RW impedances.

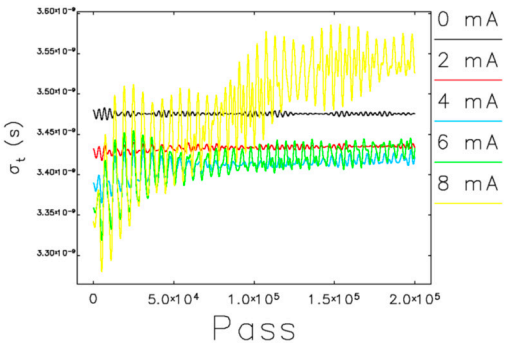

Figure 9: Bunch length vs. number of turns for different single-bunch currents with SC+GM+RW impedances.

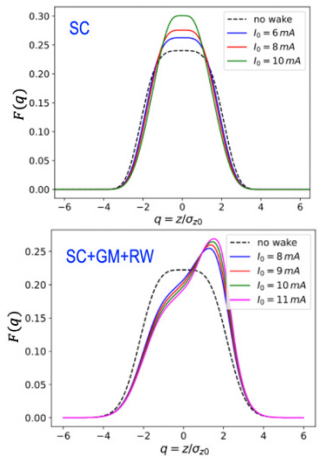

Figure 10: Beam profiles at various single-bunch currents for the LSC (left plot) and SC+GM+RW (right plot) impedances.

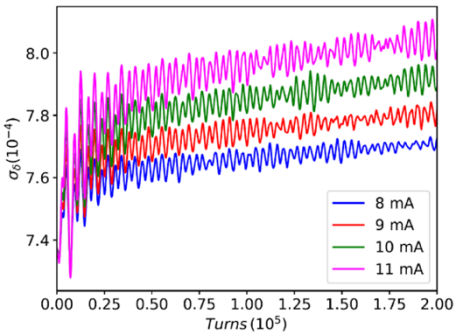

Figure 11: Energy spread vs. number of turns at various single-bunch currents using the double-RF system with combined SC+GM+RW impedances.

ISBN: 978-3-95450-261-5 ISSN: 2673-7000 doi: 10.18429/JACoW-NAPAC2025-THYD01

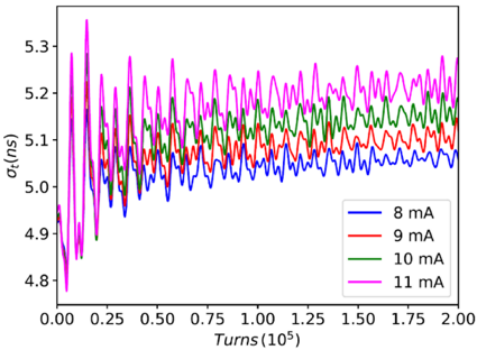

Figure 12: Bunch length vs. number of turns at various single-bunch currents using the double-RF system with combined SC+GM+RW impedances.

To cross-check the effect of the second harmonic cavity on beam dynamics, a beam experiment was performed at RHIC, which demonstrated increased bunch length and improved beam stability under a dual-RF configuration [14].

TRANSVERSE BEAM STABILITY

Work on vertical beam stability in the Hadron Storage Ring (HSR) at injection energy is ongoing, with both linear and nonlinear space charge impedances under active investigation [15]. The horizontal space charge (SC) impedance, averaged over Gaussian beam distribution, is given by

$$Z_{x,SC} = -\frac{Z_0 C}{4\pi\beta\gamma_0^2\sigma_x(\sigma_x+\sigma_y)} \tag{4}$$

The Eq. 4 is derived from the nonlinear space charge force in the round beam limit with a Gaussian transverse distribution. The transverse force, which includes both electric and magnetic components, is given by

$$(E+\mathbf{v}\times\mathbf{B})_x = \frac{Z_0 I}{2\pi\beta\gamma_0^2}\frac{(x-\bar{x})}{(x-\bar{x})^2+(y-\bar{y})^2} \times\left(1-\exp\left[-\frac{(x-\bar{x})^2+(y-\bar{y})^2}{2\sigma^2}\right]\right) \tag{5}$$

Here, σ represents the RMS transverse beam size (assuming $\sigma_x = \sigma_y = \sigma$ for around beam), Z_0 is the impedance of free space, C is the ring circumference, x and $\bar{x}$ denote the particle and centroid horizontal positions, respectively.

The effect of nonlinear transverse space charge (TSC) has been studied using a newly implemented algorithm in ELEGANT [8]. Analysis indicates that the beam becomes vertically unstable at the nominal cooled emittance of $\varepsilon_x\gamma_0 \approx 0.5$ μm and $\varepsilon_y\gamma_0 \approx 0.3$ μm. To mitigate this instability, high chromaticity (+6/+6) and RHIC-style octupole magnets [16] were introduced for tracking. The beam remained unstable under these conditions, and to mitigate the instability, the horizontal emittance was increased to $\varepsilon_x\gamma_0 \approx 3$ μm, keeping ε_y the same. The results, including tune shifts derived from both linear and nonlinear TSC impedances, are presented in Fig. 13. The dashed line is the central tune shift based on peak density with TSC impedances of $Z_{sc,x} = 90\ M\Omega/m$ and $Z_{sc,y} = 300\ M\Omega/m$. Eq. 4 for linear space charge gives values roughly half as large. Dots represent tracking results of tune distribution within the bunch over the final three turns (of 50k turns) at 3 mA single-bunch current.

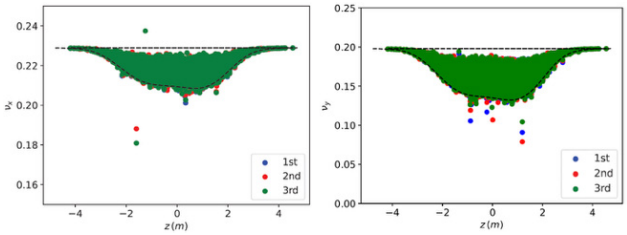

Figure 13: Tune distribution within the bunch over the final three turns (out of 50k total). Dots represent tracking results with TSC and longitudinal and transverse GM+RW impedances. The dashed line shows the analytical prediction from the linear TSC impedance.

Additionally, the sign of the octupole cross-term plays a critical role: a positive sign partially compensates for the TSC-induced tune shift, bringing the tune closer to its bare value, while a negative sign enhances the shift, potentially enhancing the instability [17,18].

CONCLUSION

The presented results for the proton beam in the HSR at injection energy based on Haissinski equilibrium analysis and particle tracking simulations using the current longitudinal impedance model (SC + GM + RW) - suggest that the beam is expected to be longitudinally single-bunch stable at the required single bunch current of 3.5 mA. While the exact instability threshold is not sharply defined with the dual-RF system, simulations up to 11 mA show no clear signs of microwave instability, supporting confidence in operational stability at the nominal intensity with an energy spread close to the design requirement. Ongoing work on transverse beam stability at injection energy focuses on understanding the effects of TSC impedance combined with the geometric and resistive wall impedance budget. A key objective is to quantify the tune shift induced by nonlinear TSC impedance within the context of the HSR lattice, considering its effect to understand the global impact on beam stability.

The author thanks M. Blaskiewicz, P. Baxevanis, X. Gu, G. Wang, A. Burov, A. Fedotov, V. Ptitsyn, M. Borland and R. Lindberg for stimulating discussions and their contributions to this subject.

REFERENCES

[1] *Electron-Ion Collider Preliminary Design Report 2025*, Brookhaven National Laboratory, Upton, NY, and Jefferson Lab, Newport News, VA, 2025.

[2] A. V. Fedotov, D. Kayran, and S. Seletskiy, "Accelerator Physics Requirements for Electron Cooler at the EIC Injection Energy," in *Proc. COOL2023*, Montreux, Switzerland, Oct. 2023, pp. 1-4. doi:10.18429/JACoW-COOL2023-MOPAM2R1

[3] I. Zagorodnov, "Indirect methods for wake potential integration," *Phys. Rev. Spec. Top. Accel Beams*, vol. 9, no. 10, p. 102002, Oct. 2006. doi:10.1103/physrevstab.9.102002

ISBN: 978-3-95450-261-5 ISSN: 2673-7000 doi: 10.18429/JACoW-NAPAC2025-THYD01

[4] I. Zagorodnov, ECHO3D, echo4d.de

[5] W. Bruns, GdfidL, www.gdfidl.de

[6] A. Burov, "Head-tail modes for strong space charge," *Phys. Rev. Spec. Top. Accel Beams*, vol. 12, no. 4, p. 044202, Apr. 2009. doi:10.1103/physrevstab.12.044202

[7] A. Burov, "Longitudinal modes of bunched beams with weak space charge," *Phys. Rev. Accel. Beams*, vol. 24, no. 6, p. 064401, Jun. 2021. doi:10.1103/physrevaccelbeams.24.064401

[8] M. Borland, *ELEGANT: A flexible SDDS-compliant code for accelerator simulation*, Advanced Photon Source, Argonne National Laboratory, Lemont, IL, USA, Rep. ANL/APS/LS-287, 2000.

[9] M. Blaskiewicz, *The TRANFT user's manual*, Brookhaven National Laboratory, Upton, NY, USA, Rep. BNL-77074-2006-IR, 2006.

[10] A. W. Chao, *Physics of Collective Beam Instabilities in High Energy Accelerators*, New York: Wiley, 1993

[11] P. Baxevanis, *EIC hadron ring longitudinal stability simulations at injection*, Brookhaven National Laboratory, Upton, NY, USA, Rep. BNL-226418-2024-TECH, EIC-ADD-TN-114, 2024.

[12] A. Piwinski, *Bunch lengthening and power losses due to the vacuum chamber walls*, DESY, Hamburg, Germany, Rep. 72/72, 1972.

[13] R. Lindberg, "Note on the Haissinski equilibrium for space charge impedance," Argonne National Laboratory, Lemont, IL, USA, 2024, unpublished.

[14] D. Kayran *et al.*, *Injection studies for the EIC with dual RF system*, Brookhaven National Laboratory, Upton, NY, USA, Rep. APEX 24-06, 2024.

[15] P. Baxevanis, M. Blaskiewicz, and A. Blednykh, "Single-Bunch Instabilities Driven by Space Charge During Low-Energy Cooling at Injection in the EIC Hadron Storage Ring," presented at NAPAC'25, Sacramento, CA, USA, Aug. 2025, paper TUP090, this conference.

[16] S. Peggs *et al.*, *Resonance island jump theory for the HSR*, Brookhaven National Laboratory, Upton, NY, USA, Rep. BNL-224979-2023-TECH; EIC-ADD-TN-077, 2023. doi:10.2172/2205642

[17] M. Blaskiewicz, "Transverse stability with nonlinear space charge," *Phys. Rev. Spec. Top. Accel Beams*, vol. 4, no. 4, Apr. 2001. doi:10.1103/physrevstab.4.044202

[18] M. Blaskiewicz and K. Mernick, "Instabilities and Space Charge," in *Proc. HB'14*, East Lansing, MI, USA, Nov. 2014, paper WEO1LR01, pp. 235-239.